Supplementary Information

Trans-membrane piezoelectric activation of peroxymonosulfate for effective control of waterborne antibiotic resistance dissemination

*Yang Yu, Lianyu Liu, Yiqiao Xie, Wei Huang, Hai Liu, Xiaotu Liu and Da Chen**

Supplementary Notes

Materials. Polytetrafluoroethylene (PTFE) aqueous dispersion (60wt%, FR301B) was purchased from 3F New Materials Co. Ltd. (China). Zinc acetate dehydrate ($Zn(CH_3COO)_2•2H_2O$), anhydrous ethanol (EtOH), phosphate buffer saline (PBS), methanol (MeOH), Isopropanol (IPA), superoxide dismutase (SOD), L-histidine (L-his), potassium iodide (KI), potassium peroxymonosulfate ($KHSO_5•0.5KHSO_4•0.5K_2SO_4$, PMS), tertiary butyl alcohol (TBA), potassium dichromate ($K_2Cr_2O_7$), ^{18}O-labelled DI water and sodium thiosulfate ($Na_2S_2O_3$) were purchased from Aladdin Chemical Reagent Co. Ltd. (China). The 5,5'-dimethyl-1-pyrroline-n-oxide (DMPO) and dimethylsulfoxide (DMSO) were purchased from Dojindo Laboratories (Japan) and Sigma-Aldrich (China), respectively. Luria-Bertani (LB) broth and agar were obtained from Beijing Aoboxing Bio-Tech Co. Ltd. (China). SYBR® Green I (SGI) and propidium iodide (PI) were purchased from Invitrogen AG (Switzerland). SanPrep Column DNA Gel Extraction Kit and Ezup Column Bacteria Genomic DNA Purification Kit were purchased from Sangon Biotech (China). *Escherichia coli* (bio-56954) containing plasmids encoded with bla_{TEM}-1 and *aac(3)-II* genes was chosen as representative antibiotic resistant bacteria in this study (purchased from Beijing Baiou Bowei Bio-Tech Co. Ltd., China), due to its widespread distributions in aquatic environments. As one of the mobile genetic elements containing antibiotic resistance genes (ARGs), plasmids pUC57 encoded with bla_{TEM}-1 (purchased from Beijing Baiou Bowei Bio-Tech Co. Ltd., China) were employed as model extracellular ARGs.

Fabrication of ZnO nanorods. The ZnO nanorods were synthesized through hydrothermal reactions. In brief, 0.4395 g of $Zn(CH_3COO)_2•2H_2O$ was added into 20-mL anhydrous ethanol under mechanical stirring for 2 h to form homogeneous solution. After 40 mL NaOH solution (0.5 M in ethanol) was added under sonication for 30 min, the mixture was transferred into a Teflon-lined stainless-steel autoclave (100 mL) and kept at 150 ^oC for 24 h. The obtained white precipitate was washed and centrifuged with deionized water and ethanol for at least five times to remove residual reagents. Finally, the precipitate was dispersed into ethanol and treated by sonication for 3 h prior to freeze-drying.

Piezoelectric membrane filtration apparatus. The performance of piezoelectric PMS activation by PTFE-ZnO nanofiber membrane in the elimination of ARB and ARGs was evaluated using a lab-scale cross-flow membrane filtration apparatus as illustrated in Supplementary Fig. 1. The effective area of the PTFE-ZnO nanofiber membrane was 12.56 cm^2. During filtration, the ARB suspension solution or plasmid reaction solution was pumped into the water inlet of filtration apparatus through tube A, while the PMS solution or PBS solution was pumped into the water inlet of filtration apparatus through tube B. The peristaltic pump was used to drive the mixture from tube A or B to flow across the membrane surface in the filtration apparatus. Under hydraulic pressure, a part of stream with low concentration of ARB cells would permeate through the membrane and can be collected from the permeate outlet of the filtration apparatus. Due to the membrane sieving effect, the majority of stream with concentrated ARB cells would be collected from the retentate outlet of the filtration apparatus.

Long-term performance and reusability of the membrane. For the continuous 3-cycle operation process, the membrane was only rinsed by deionized water before the next cycle. The samples were taken from the permeate in different time intervals, and the abundance of tARGs in the permeate were determined by using qPCR.

Preparation of *E. coli* suspension and regrowth analysis. The *Escherichia coli* (bio-56954) with amoxicillin resistance gene (bla_{TEM}-1) and gentamicin resistance gene (*aac(3)-II*) were inoculated from glycerol samples into 20-mL sterile LB broth under shaking (37 ºC and 150 rpm) for 12 h to reach the stationary phase. The ARB cells were harvested by centrifugation, washed with sterile PBS solution and resuspended into a PBS solution to obtain ARB stock solution with the cell concentration of ~10^9 colony-forming unit per milliliter (CFU·mL^{-1}) through adjusting the solution absorbance at λ of 600 nm.

The regrowth experiments were carried out to evaluate self-repairing ability of ARB after treatment. An aliquot of 10 μL sample taken from the retentate or permeate of piezoelectric PMS activation by PTFE-ZnO nanofiber membrane filtration was added into 20-mL liquid LB broth and incubated at 37 ºC and 150 rpm for 72 h. During the regrowth period, 1-mL sample was collected at three time intervals (24 h, 48h and 72h) and serially diluted with PBS solution. After that, an aliquot of 100 μL was spread on the BL agar plate for viable cell counting.

Preparation of plasmid solutions. Plasmids pUC57 encoded with bla_{TEM}-1 gene were chosen as the model extracellular ARGs and dispersed well into the PBS solution at room temperature. The abundance of target ARGs in plasmid stock solution was determined with qPCR. The reaction solution with a gene concentration of ~10^6 gene copy number per milliliter (copies·mL^{-1}) was prepared by diluting plasmid stock solution with PBS solution. The plasmid stock solution was stored at -20 ºC, and the reaction solution was freshly prepared prior to use.

Degradation of plasmid. Plasmid pUC57 encoded with bla_{TEM}-1 was chosen as the model eARGs (Details available in *SI Appendix*). Sample DNA was collected by using SanPrep Column DNA Gel Extraction Kit (Sangon Biotech) and the abundance of bla_{TEM}-1 gene was quantified by qPCR and semi-quantified by gel electrophoresis (Details available in *SI Appendix*) at 100 V for 30 min using the gel electrophoresis system (Benchmark Scientific).

ARB inactivation and ARGs removal from tap water. In order to evaluate the performance of the proposed system on the ARB inactivation and ARGs elimination from the real water or co-existing natural organic matters, the ARB working solution was prepared by diluting ARB stock solution with tap water. Other procedures were the same as those used in the reduction of ARB and ARGs in filtration mode.

Estimation of fluid retention time in zone 1 and zone 2. During filtration, the majority of influent will flow across the membrane and then discharge from the retentate outlet. Meanwhile, a portion of stream will permeate through the membrane. The retention time in zone 1 was estimated as follows:

$$t_1 = \frac{V_1}{Q_r} = \frac{S \times h_1}{Q_r} \quad (1)$$

where t_1 is the retention time of fluid in zone 1 during the filtration (min), S is the effective area of membrane (cm^2), h_1 is the height of water layer on the membrane surface (cm), which can be obtained from the inlet plate of membrane module, and Q_r is the flow rate of retentate ($mL \cdot min^{-1}$), which is determined by recording the volume of retention in a given time interval.

For the trans-membrane piezocatalytic process (zone 2), the retention time was calculated as follows:

$$t_2 = \frac{V_2}{Q_p} = \frac{S \times h_2 \times P}{Q_p} \quad (2)$$

where t_2 is the retention time of fluid in zone 2 during the filtration (min), S is the effective area of membrane (cm^2), h_2 is the thickness of the membrane (cm), which can be obtained by cross-sectional SEM image of the membrane, P is the total porosity of the membrane (%), which is determined by mercury intrusion porosimetry, and Q_p is the flow rate of permeate ($mL \cdot min^{-1}$), determined by recording the volume of permeate in a given time interval.

Estimation of ARGs reduction rates. The ARGs degradation during the piezoelectric PMS activation by PTFE-ZnO nanofiber membrane filtration is controlled by ROS-dominant reactions. Therefore, the reduction rate constants of ARGs in zone 1 and zone 2 can be simulated by the below equation:

$$k = -\ln(C/C_0)/t \quad (3)$$

where C_0 and C represent the abundance of ARGs before and after degradation in specific reaction zone ($mg \cdot L^{-1}$), respectively, and t is the retention time in zone 1 or 2 (min).

The concentration of ARGs in the retentate outlet is not only determined by the piezocatalytic process in zone 1, but also the permeation of ARGs through the membrane. Therefore, the reduction rate of ARGs degradation in zone 1 was estimated by a modified filtration process in which the small mesh below the membrane was replaced by a nonporous plate to prevent the permeation. The flow rate of stream was adjusted to be the same value of retentate in normal filtration process (Q_r). The abundances of iARGs and eARGs in the feed solution and samples from the retentate outlet were determined by qPCR.

If the valve of retentate outlet was closed, the concentration of ARB near the membrane surface would be gradually increased with the operation time, due to the membrane sieving effect, while the

abundance of ARGs in the permeate is also elevated along with time. Therefore, the approach used for zone 1 would not be suitable for estimating the ARGs reduction rate in zone 2. We treated the permeation process as an independent step followed by the ROS-dominant piezocatalytic process in zone 1, and the stable concentration of ARGs near the membrane was estimated according to the reduction rate in zone 1. Then, the abundance of ARGs that enter into the membrane was approximately calculated according to the rejection efficiency of membrane toward ARB and plasmids (Table S2). Finally, the ARGs reduction rate in zone 2 was estimated based on Eq. 3.

Zn leaching of the membrane during the treatment. The samples were taken in different time intervals of the first cycle operation process. After the complete digestion by the mixture of nitric acid and hydrochloric acid, the concentration of Zn ions was measured by inductively coupled plasma-mass spectroscopy (ICP-MS).

PMS activation efficiency. The residual concentrations of PMS in the retentate and permeate were determined as follows: The samples (1 mL) were taken from the retentate and permeate after the system was stably carried out for at least 30 min. Then, the samples were added to a 10-mL glass tube containing 1 mL of KI/$NaHCO_3$ (0.5 $g \cdot L^{-1}$) solution, transferred to a volumetric flask, diluted with deionized water to the predetermined volume. The resulting solution was equilibrated for 15 min. Finally, the concentration of PMS was analyzed at 352 nm by UV-Vis spectrophotometer.

Horizontal gene transfer (HGT) analysis. The *E. coli* bio-82271, containing the pRARE plasmid that carries the chloramphenicol resistance gene, was employed as the model environmental bacterial strain (EBS). The samples (1 mL) were taken from the feed solution, retentate and permeate after the system was stably conducted for 30 min. Then, the samples and 1-mL EBS suspension with the abundance of ~10^7 $CFU \cdot mL^{-1}$ were added into 100-mL LB broth, followed by incubation for 12 h at 37 °C. After that, the mixture was serially diluted and spread on LB agar plates containing different antibiotics to determine the abundance of ARB, EBS, and HGT cells. Ampicillin (100 $mg \cdot L^{-1}$) and gentamicin (40 $mg \cdot L^{-1}$) were supplemented with ARB selective plates, and chloramphenicol (30 $mg \cdot L^{-1}$) was supplemented with EBS selective plates. The HGT cells were selected by plates containing 100 $mg \cdot L^{-1}$ ampicillin, 40 $mg \cdot L^{-1}$ gentamicin, and 30 $mg \cdot L^{-1}$ chloramphenicol. The HGT frequencies were calculated using the following equation:

$$HGT\ frequency = \frac{HGT\ cell\ abundance}{EBS\ abundance} \quad (4)$$

Determination of piezoelectric current. The piezoelectric current was monitored by electrochemical workstation (CHI760E, CH Instruments) with a three-electrode system. The PTFE-ZnO nanofiber membrane was fixed into the filtration apparatus without the inlet plate in order to expose the membrane surface to the background solution. A copper ring was sandwiched between the membrane and sealing rubber ring and then

connected with the working electrode. The modified filtration apparatus was placed into a beaker containing the background solution. The peristaltic pump was used to drive the solution to flow through the membrane and return back to the beaker. The counter and reference electrodes were also immersed into the solution during the current monitoring process.

Identification of ROS generation routes. The pathways for the ROS generation in the piezoelectric PMS activation during PTFE-ZnO nanofiber membrane filtration were identified via a series of batch experiments along with *a prior* knowledge on the ROS generation [1-3].

(1) Electron spin resonance (ESR) analysis of •OH, $•O_2^-$and $^1O_2$ after the quenching of piezo-induced electron (e^-)

A piece of PTFE-ZnO nanofiber membrane with an area of 1 cm^2 and a mixture of potassium dichromate (the electron scavenger) and PMS with the relative molar ratio of 20:1 were added into 1-mL deionized (DI) water. DMPO (50 mM), DMPO/DMSO (50 mM/100 mM) or TEMP (50 mM) was added to detect the signals of hydroxyl radical (•OH), superoxide radical ($•O_2^-$) or singlet oxygen ($^1O_2$) by ESR, respectively. After ultrasonication for 5 min, the samples were taken to determine the ESR signal intensity of DMPO-•OH, DMPO/DMSO-$•O_2^-$ or TEMP-$^1O_2$ after the quenching of piezo-induced electron. The ESR signal intensity before quenching was also determined without the addition of potassium dichromate.

(2) ESR analysis of $•O_2^-$ and $^1O_2$ after the quenching of piezo-induced hole (h^+)

A piece of PTFE-ZnO nanofiber membrane with an area of 1 cm^2 and a mixture of KI (the scavenger of piezo-induced h^+) and PMS with the relative molar ratio of 20:1 were added into 1-mL DI water. DMPO/DMSO (50 mM/100 mM) or TEMP (50 mM) was added to detect the signals of superoxide radical ($•O_2^-$) or singlet oxygen ($^1O_2$) by ESR, respectively. After ultrasonication for 5 min, the samples were taken to determine the ESR signal intensity of DMPO/DMSO-$•O_2^-$ or TEMP-$^1O_2$ after the quenching of piezo-induced hole. The ESR signal intensity before quenching was also determined without the addition of KI.

(3) ESR analysis of $•O_2^-$ with different concentrations of PMS and dissolved O_2

A piece of PTFE-ZnO nanofiber membrane with an area of 1 cm^2 and PMS (1, 5 or 10 mM) were added into 1-mL DI water. DMPO/DMSO (50 mM/100 mM) was added to detect the signals of superoxide radical ($•O_2^-$) by ESR. After ultrasonication for 5 min, the samples were taken to determine the ESR signal intensity of DMPO/DMSO-$•O_2^-$ under different PMS concentrations. To evaluate the effect of dissolved oxygen concentration, the DI water was aerated by N_2, air or O_2 for at least 1 h, and then a piece of PTFE-ZnO nanofiber membrane with an area of 1 cm^2 and 5 mM PMS were added. After ultrasonication for 5 min, the

samples were taken to determine the ESR signal intensity of DMPO/DMSO-•O_2^- under different concentrations of dissolved oxygen.

(4) ESR analysis of •O_2^- and $^1O_2$ with the addition of ^{18}O-labelled DI water

A piece of PTFE-ZnO nanofiber membrane with an area of 1 cm^2 and 5 mM PMS were added into a mixture of 0.5-mL DI water and 0.5-mL ^{18}O-labelled DI water. DMPO/DMSO (50 mM/100 mM) or TEMP (50 mM) was added to detect the signals of superoxide radical (•O_2^-) or singlet oxygen ($^1O_2$) by ESR, respectively. After ultrasonication for 5 min, the samples were taken to determine the ESR signal intensity of DMPO/DMSO-•O_2^- or TEMP-$^1O_2$ with the addition of ^{18}O-labelled DI water.

(5) ESR analysis of $^1O_2$ after the quenching of •OH and •O_2^-

A piece of PTFE-ZnO nanofiber membrane with an area of 1 cm^2 was added into 1-mL DI water, followed by addition of a mixture of SOD (the scavenger of piezo-induced •O_2^-), IPA (the scavenger of •OH) and PMS with the relative molar ratio of 20:20:1. TEMP (50 mM) was added to detect the signals of singlet oxygen ($^1O_2$) by ESR. After ultrasonication for 5 min, the samples were taken to determine the ESR signal intensity of TEMP-$^1O_2$ after the quenching of •OH and •O_2^-. The ESR signal intensity before quenching was also determined without the addition of SOD and IPA.

(6) Determination of H_2O_2 after the quenching of piezo-induced electron (e^-)

A piece of PTFE-ZnO nanofiber membrane with an area of 1 cm^2 and a mixture of potassium dichromate (the electron scavenger) and PMS with the relative molar ratio of 20:1 were added into 1-mL DI water. After ultrasonication for 5 min, the samples were taken to determine the concentration of H_2O_2 using a modified ammonium metavanadate spectrophotometric method [4].

As shown in Supplementary Figure 20A, the quenching of piezo-induced electron (e^-) resulted in decreasing ESR signal intensity of DMPO-•OH, suggesting the existence of Eq. 1 and 2. By contrast, the ESR signal intensities of DMPO/DMSO-•O_2^- and TEMP-$^1O_2$ were increased. This indicates the likelihood of Eq. 4, 7 and 8, as the quenching of e^- could result in more separated piezo-induced holes (h^+) participating in the generation of $^1O_2$ and •O_2^- via these pathways. The occurrence of Eq. 7 and 8 was further confirmed by reduced ESR signal intensity of TEMP-$^1O_2$ after quenching •OH and •O_2^- (Supplementary Figure 20B). The ESR signal intensity of DMPO/DMSO-•O_2^- and TEMP-$^1O_2$ nearly disappeared after quenching h^+ (Supplementary Figure 21A and B), indicating the important role of Eq. 4 in •O_2^- formation. While Eq. 4 also suggests that elevated PMS concentrations could promote •O_2^- generation, the ESR signal intensity of DMPO/DMSO-•O_2^- was decreased along with the increase of PMS concentration (Supplementary Figure 21C), likely attributable to the transformation from •O_2^- to $^1O_2$ via Eq. 6. In addition, although Eq. 3 was

demonstrated by the promotion of $^1O_2$ generation along with increasing dissolved oxygen (Supplementary Figure 21D), low concentrations of dissolved oxygen in actual water suggest that Eq. 3 may only play a limited role in $^1O_2$ generation. Further, the addition of ^{18}O-labelled DI water into the system can slow down the kinetics of Eq. 5, leading to the accumulation of $\bullet O_2^-$ and reduction of $^1O_2$ (Supplementary Figure 21E and F). Meanwhile, non-detection of H_2O_2 in the system after quenching e^- suggested negligible H_2O_2 formation from $\bullet O_2^-$. Therefore, we derive above pathways (Eq. 1–8) for the ROS generation in the piezoelectric PMS activation during PTFE-ZnO nanofiber membrane filtration.

Gel electrophoresis. Gel electrophoresis was applied to verify the damage of target genes in the plasmid. The samples were taken from the feed tank, retentate outlet and permeate outlet after stable operation for 30 min. The DNA was extracted and concentrated from samples by using the SanPrep Column DNA Gel Extraction Kit. The separated gene sequence was mixed with gel-loading buffer and then loaded in 1.0% agarose gel with SYBR Green I. The gel electrophoresis was conducted in 1× TAE solution at 100 V for 30 min using a gel electrophoresis instrument (DYY-12C, China). The bands were visualized under UV irradiation by using a ChemiDoc EQ^{TM} UV Transilluminator (Bio-Red, USA).

qPCR analysis. The qPCR was employed to determine the abundance of ARGs using a CFX96^{TM} Real-time system. The qPCR reaction mixture contained 2-μL template DNA, 10-μL 2×SYBR Green qPCR Master Mix, 7-μL DEPC H_2O, 0.5-μL forward primer and 0.5-μL reverse primer to a total volume of 20 μL. The DNA polymerase and main reagents were provided by Sangon Biotechnology Corporation (China). The primer sets used in qPCR testing were (5'-GGT CGC CGC ATA CAC TAT TCT-3') as the forward primer and (5'- GGT TAG CTC CTT CGG TCC TC-3') as the reverse primer. The detailed protocol of qPCR analysis was programmed as follows: 95 °C for 10 min, 30 cycles of 95 °C for 30 s, and 60 °C for 30 s, followed by a melting curve for specificity verification. In each PCR run, pristine naked DNA was used as positive control, genomic DNA extracted from ARB or plasmid was used as a negative control, and nuclease-free water was used as blank control. The qPCR efficiency in the range of 90%-110% with a correlation coefficient (R^2) higher than 0.99 was used to develop a standard curve, and the extraction and qPCR analysis for each sample were conducted in triplicate.

Energy consumption calculation. The normal rated powers of ultrasonic cleaner and peristaltic pump are 180 W and 20 W, respectively. The real power of ultrasonic irradiation consumed for the reaction was assumed according to the volume ratio of bath water in ultrasonic cleaner and liquid in the reactor. Similarly, the real power of peristaltic pump used for driving piezoelectric effect of the membrane was simply assumed by the ratio of setting flow rate and maximum operable flow rate. Then, the unit energy consumption for ARGs removal can be calculated according to the absolute abundance of ARGs eliminated after the membrane filtration and corresponding power consumption.

Supplementary Figures

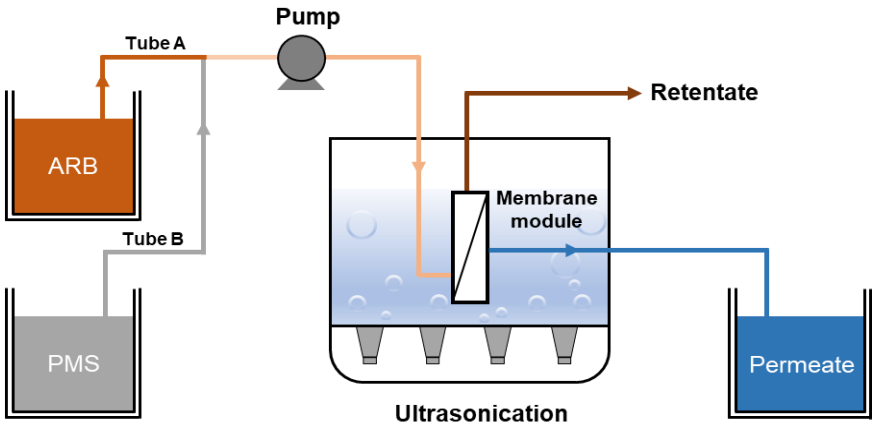

Supplementary Figure 1. Schematic illustration of piezoelectric membrane filtration system for trans-membrane PMS activation and elimination of waterborne antibiotic resistance.

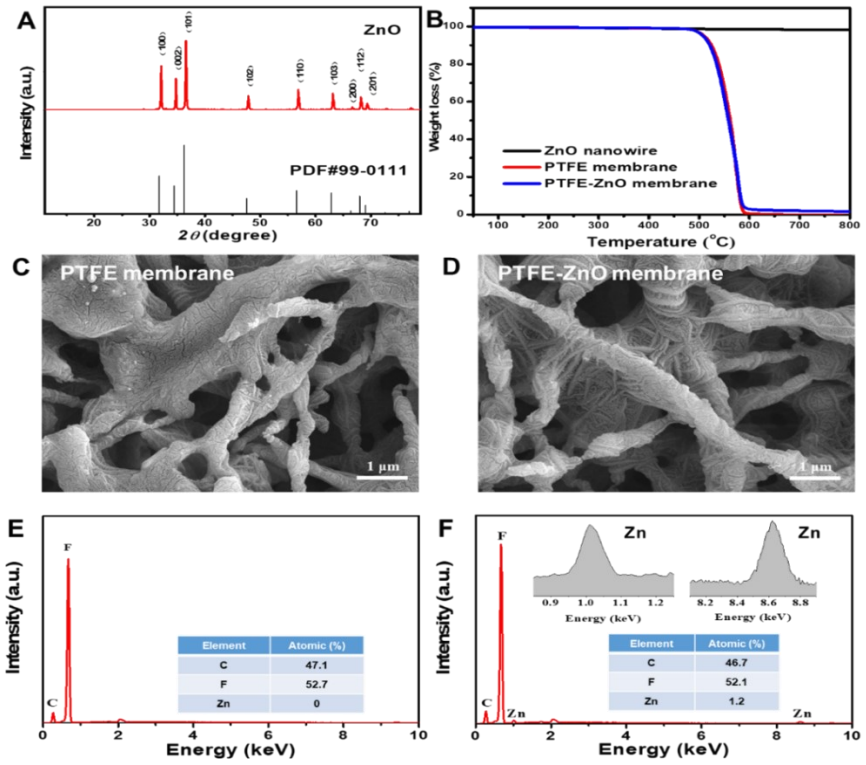

Supplementary Figure 2. Characterization of ZnO nanorods and piezoelectric membranes. (***A***) X-ray diffraction (XRD) analysis of ZnO nanorods. (***B***) Thermogravimetric analysis (TGA) of ZnO nanorods, PTFE and PTFE-ZnO nanofiber membranes. (***C, D)*** SEM images of PTFE and PTFE-ZnO nanofiber membranes, respectively. (***E, F***) Energy dispersive X-ray spectroscopy of PTFE and PTFE-ZnO nanofiber membranes, respectively.

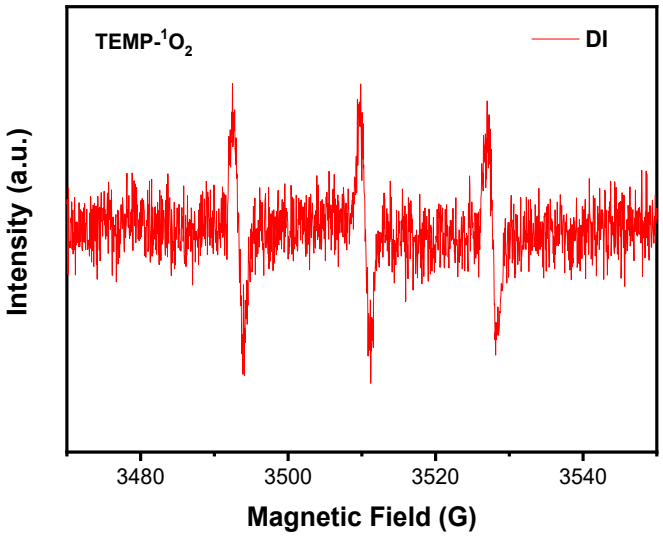

Supplementary Figure 3. ESR signals of TEMP-$^1O_2$ generated by the membrane in deionized (DI) water under ultrasonic irradiation.

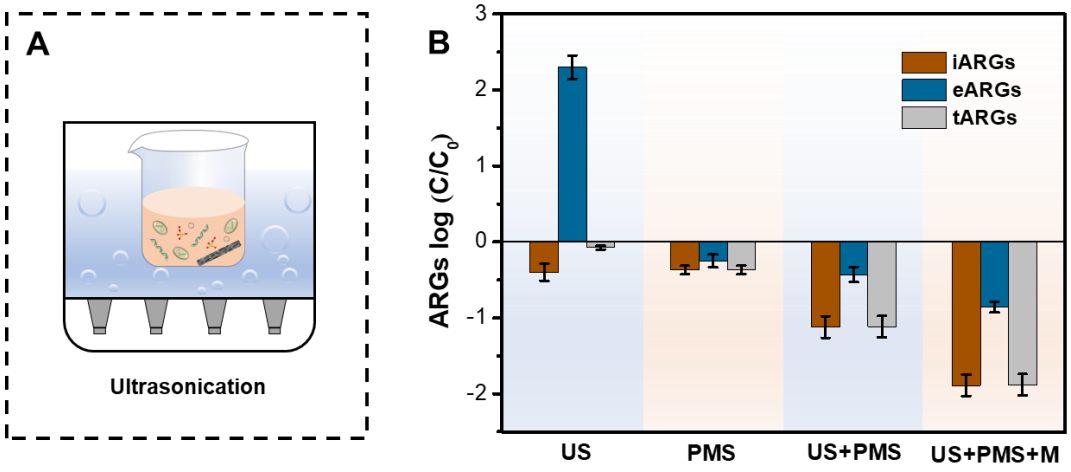

Supplementary Figure 4. Elimination of ARGs in batch study. (***A***) Schematic illustration of the batch study. (***B***) Elimination of ARGs after treatment by US, PMS, US+PMS and US+PMS+M. US: 50-mL ARB solution was ultrasound irradiated for 30 min. PMS: 50-mL ARB solution containing 1 mM PMS was stirred for 30 min. US+PMS: 50-mL ARB solution containing 1 mM PMS was ultrasound irradiated for 30 min. US+PMS+M: 50-mL ARB solution containing 1 mM PMS and a piece of PTFE-ZnO membrane with the area of 1 cm^2 was ultrasound irradiated for 30 min. Error bars represent standard deviations.

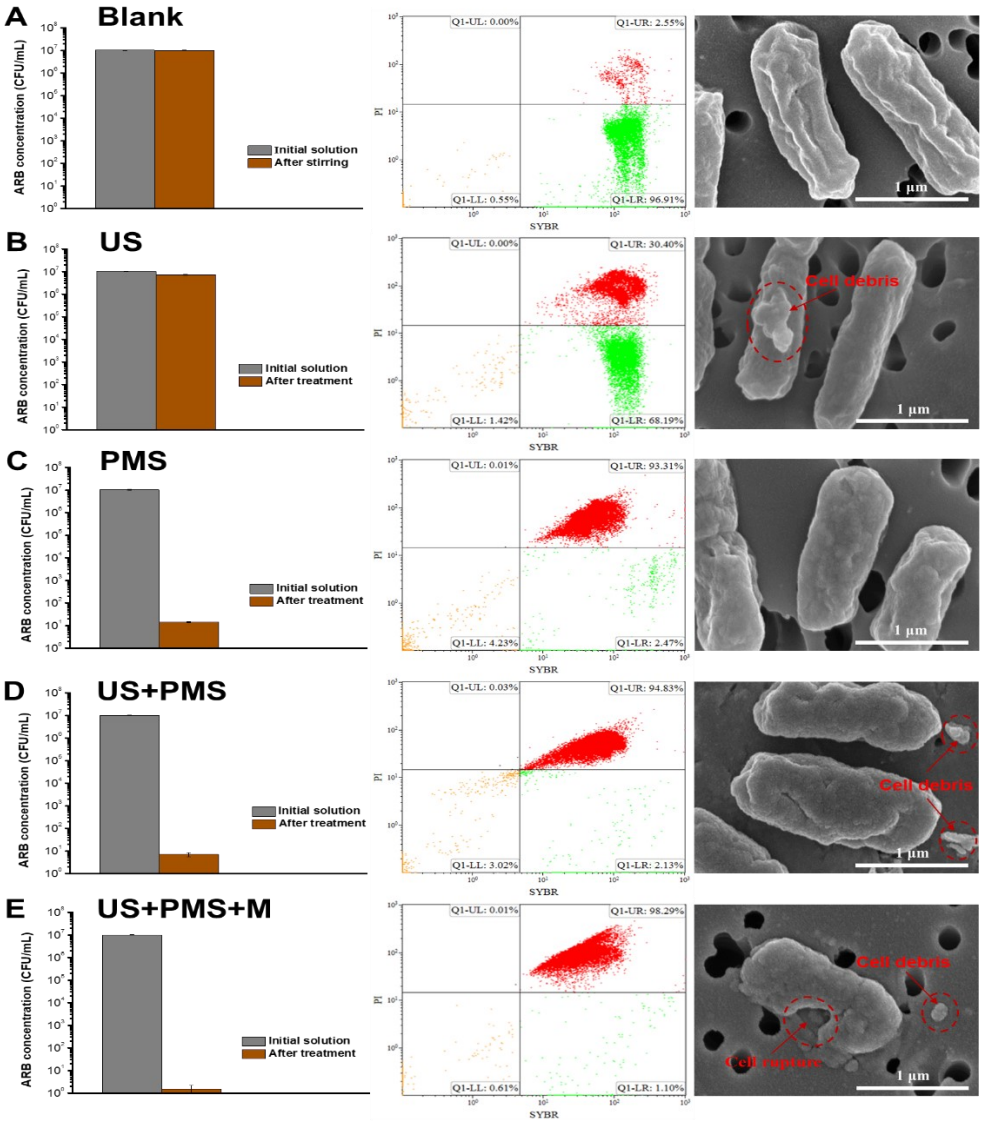

Supplementary Figure 5. Inactivation of ARB in batch study. (***A-E***) Inactivation of ARB in the blank, US, PMS, US+PMS and US+PMS+M systems, respectively. Left graphs represent post-treatment concentrations of ARB determined by the plate counting method; middle graphs summarize the intact cell count changes determined by the flow cytometry; right graphs describe the morphology change of ARB cells under SEM observation. Blank: 50-mL ARB solution was only stirred for 30 min.US: 50-mL ARB solution was ultrasound irradiated for 30 min. PMS: 50-mL ARB solution containing 1 mM PMS was stirred for 30 min. US+PMS: 50-mL ARB solution containing 1 mM PMS was ultrasound irradiated for 30 min. US+PMS+M: 50-mL ARB solution containing 1 mM PMS and a piece of PTFE-ZnO membrane with an area of 1 cm^2 was ultrasound irradiated for 30 min. Error bars represent standard deviations.

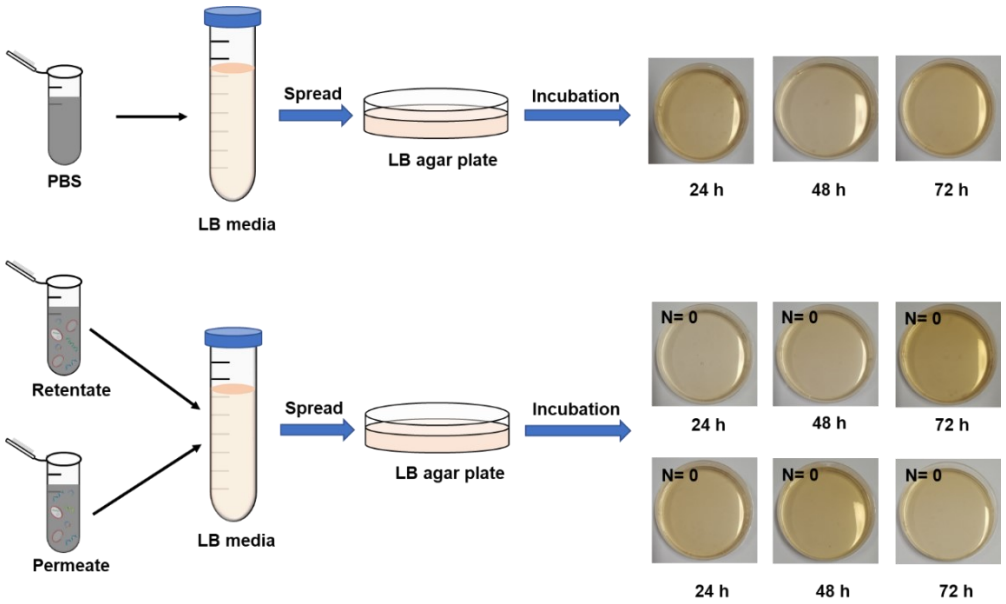

Supplementary Figure 6. Regrowth of treated ARB after incubation in LB media for 24 h, 48h and 72 h.

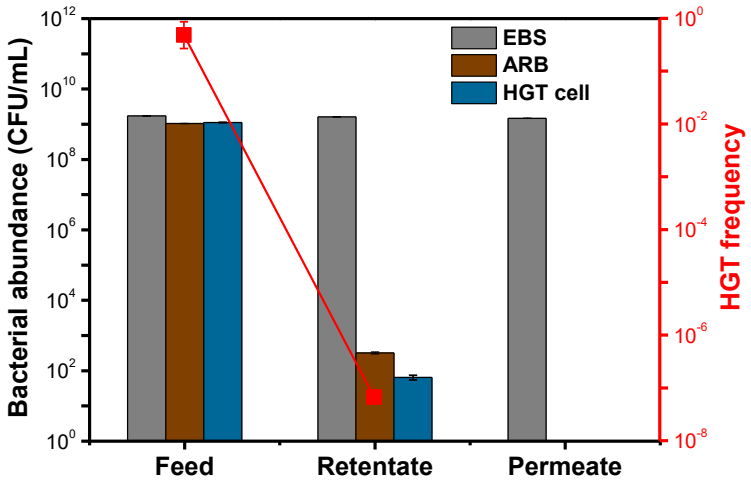

Supplementary Figure 7. HGT frequency in the feed solution, retentate and permeate.

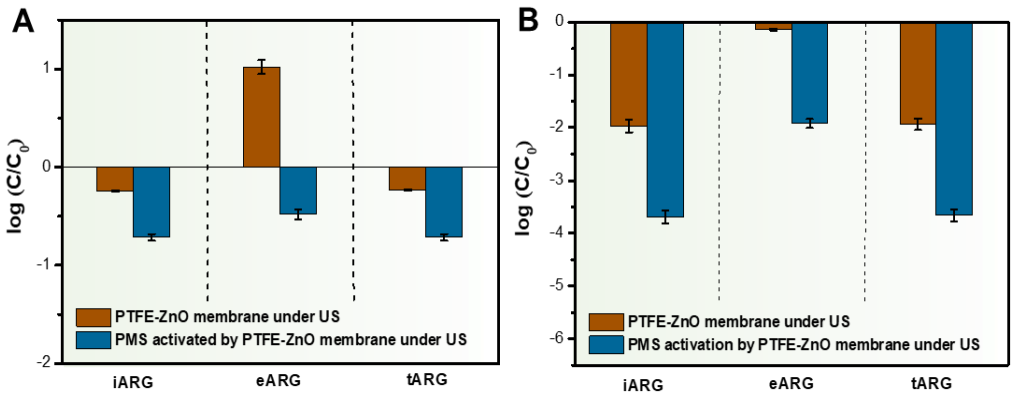

Supplementary Figure 8. Elimination of ARGs in the retentate (*A*) and permeate (*B*). The brown and blue bars represent the outcomes in two different systems: ultrasonic-driven piezoelectric PTFE-ZnO nanofiber membrane filtration without PMS activation and piezoelectric PMS activation during PTFE-ZnO nanofiber membrane filtration. The iARGs, eARGs and tARGs represent the intracellular, extracellular, and total ARGs, respectively. Error bars represent standard deviations.

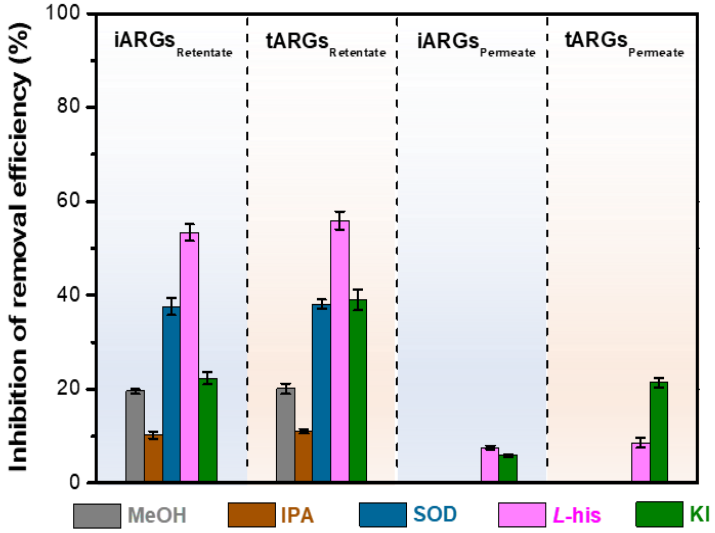

Supplementary Figure 9. Inhibition of ARGs removal by the employment of ROS quenchers. The quenchers included methanol (MeOH), isopropanol (IPA), superoxide dismutase (SOD), *L*-histidine (*L*-his) and potassium iodide (KI). Error bars represent standard deviations.

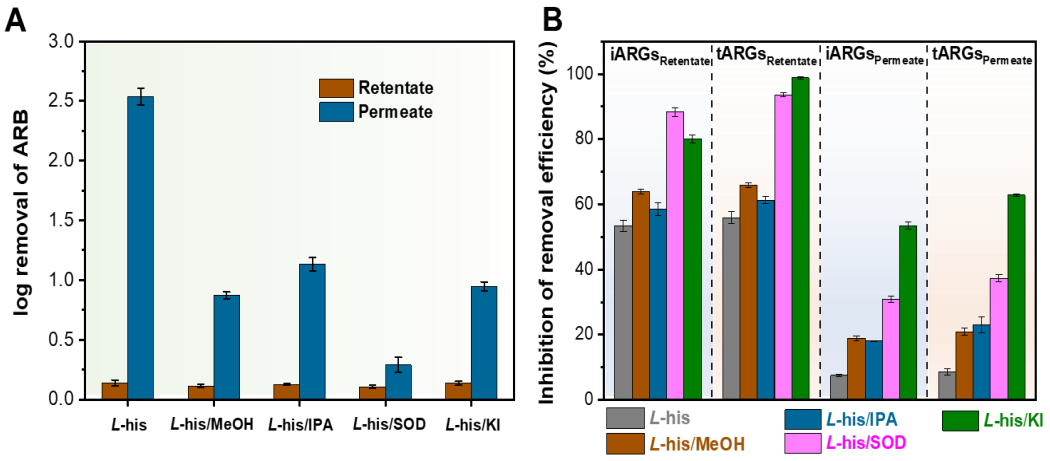

Supplementary Figure 10. Identification of the roles of other ROS in ARB inactivation and ARGs elimination when $^1O_2$ was pre-quenched by *L*-his. (***A***) ARB elimination in the retentate or permeate of piezoelectric PMS activation during PTFE-ZnO nanofiber membrane filtration. (***B***) Inhibition of ARGs removal efficiency in the retentate or permeate of piezoelectric PMS activation during PTFE-ZnO nanofiber membrane filtration. *L*-his/X (X: MeOH, IPA, SOD and KI) refers to the addition of *L*-his and X into the system together.

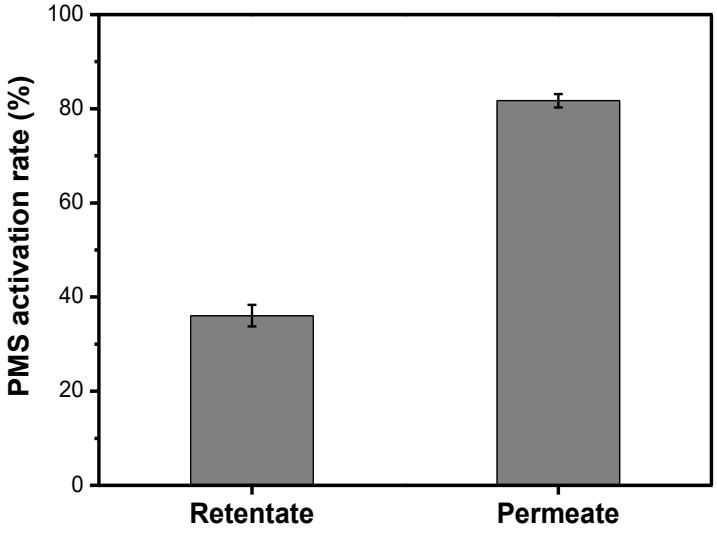

Supplementary Figure 11. PMS activation efficiency in the retentate and permeate.

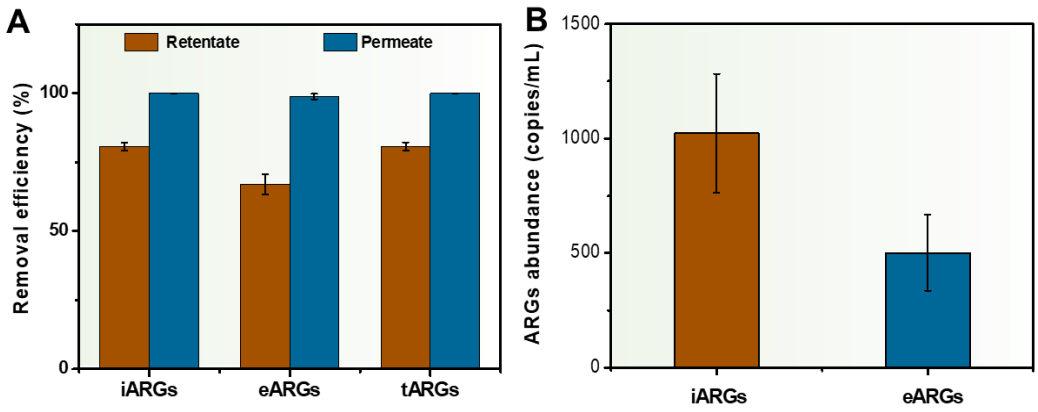

Supplementary Figure 12. Dual-zone elimination of ARGs by piezoelectric PMS activation during PTFE-ZnO nanofiber membrane filtration. (***A)*** Removal efficiencies of ARGs in the retentate and permeate. (***B***) Residual ARGs concentrations in the permeate.

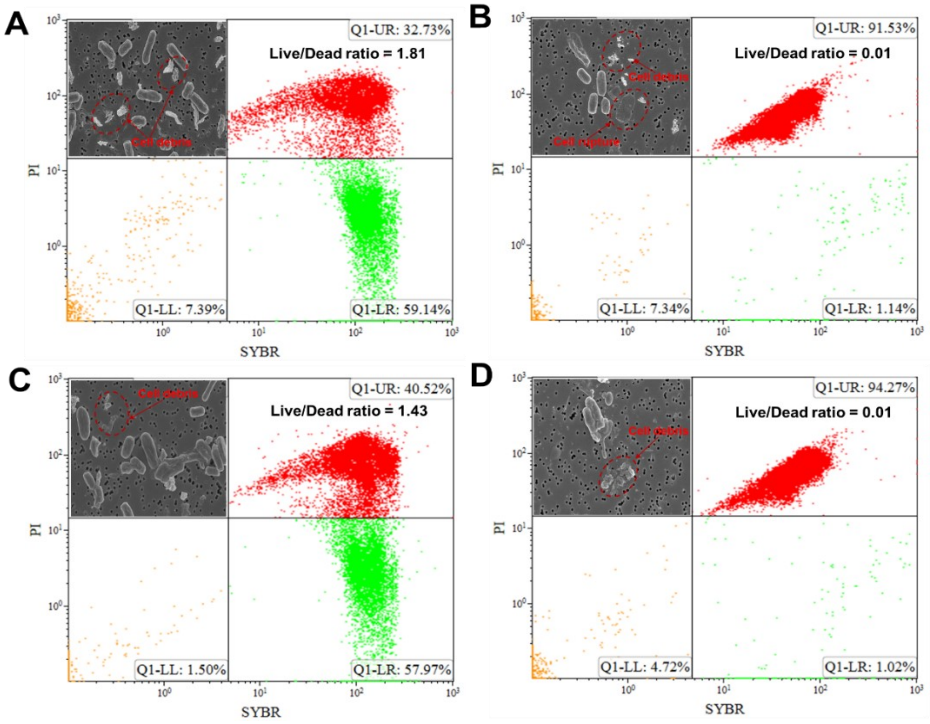

Supplementary Figure 13. Change of intact cell count and morphology of ARB. (***A, B***) Flow-cytometric density of ARB cells in the retentate and permeate of ultrasonic-driven piezoelectric PTFE-ZnO nanofiber membrane filtration without PMS activation, respectively (insert graphs: morphology of ARB cells). (***C, D***) Flow-cytometric density of ARB cells in the retentate and permeate of piezoelectric PMS activation during PTFE-ZnO nanofiber membrane filtration, respectively (insert graphs: morphology of ARB cells).

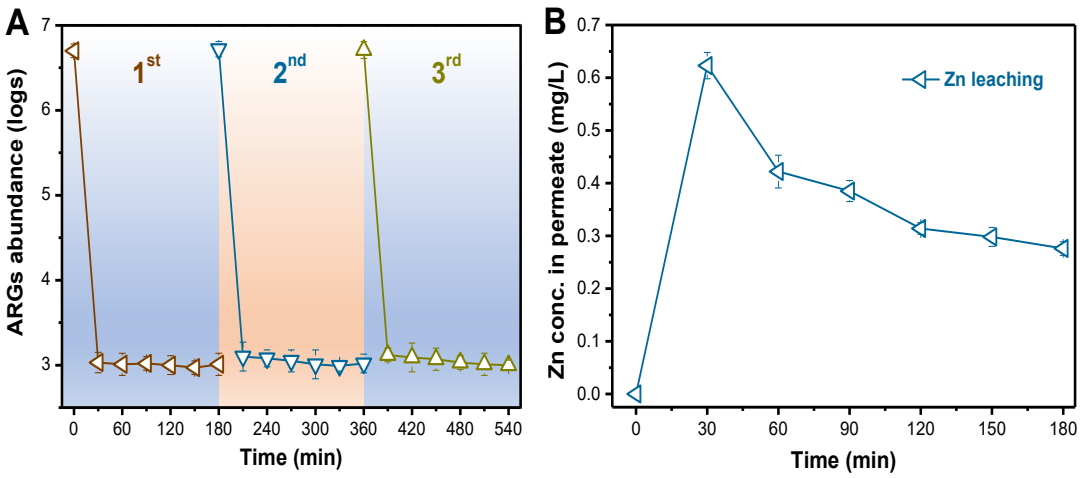

Supplementary Figure 14. Long-term performance (A) and Zn leaching (B) of the piezoelectric PTFE-ZnO nanofiber membrane. The tARGs abundance and Zn concentration in the permeate was monitored during the treatment.

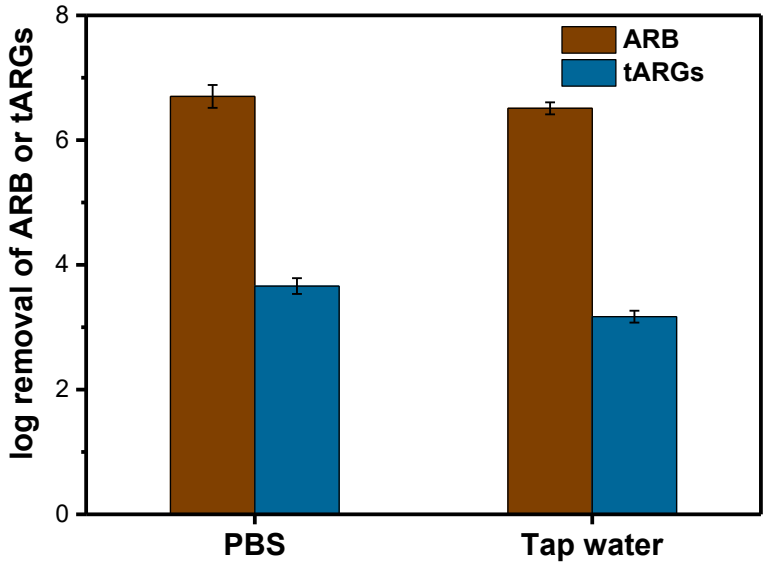

Supplementary Figure 15. ARB inactivation and tARGs removal by ultrasonic-driven piezoelectric PTFE-ZnO nanofiber membrane filtration from PBS solution and tap water.

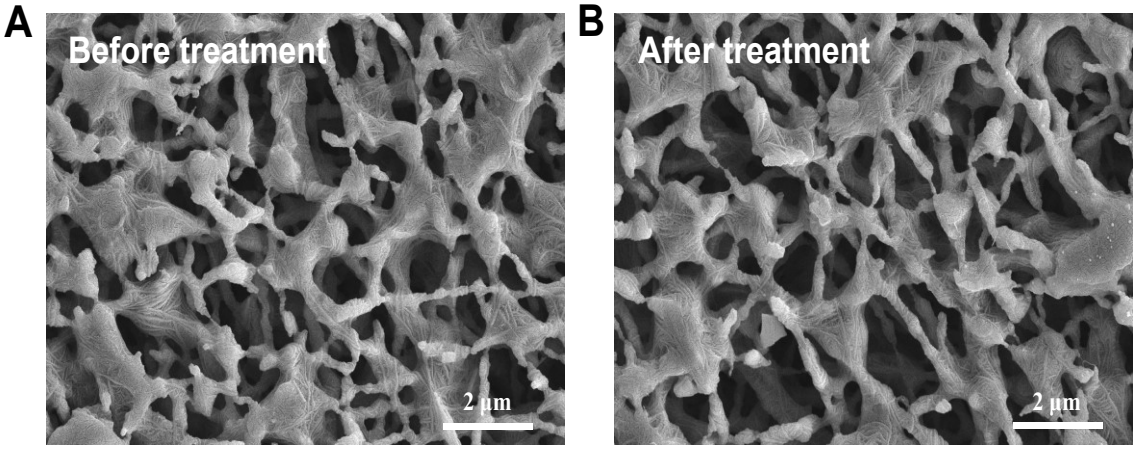

Supplementary Figure 16. Surface morphology of the membrane before and after the treatment.

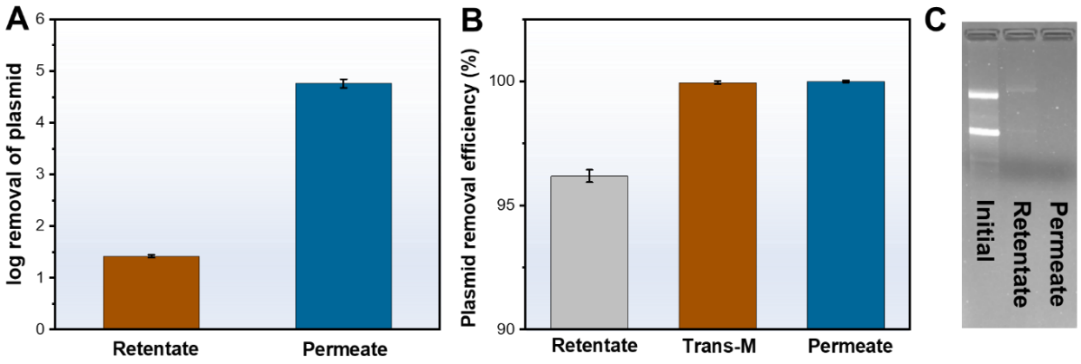

Supplementary Figure 17. Dual-zone elimination of eARGs by piezoelectric PMS activation during PTFE-ZnO nanofiber membrane filtration. (***A***) Log removal of plasmids pUC57 encoded with *bla*$_{TEM}$-1 in the retentate and permeate. (***B***) Removal efficiencies of plasmids in the retentate, during the trans-membrane transport process, and in the permeate. (***C***) Gel electrophoresis analysis of samples taken from the initial solution, retentate and permeate. Error bars represent standard deviations.

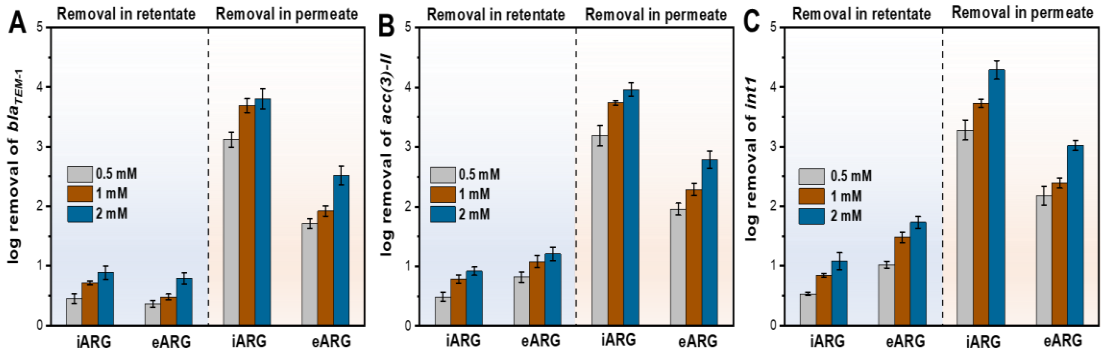

Supplementary Figure 18. Effect of PMS dosage on the dual-zone elimination. (***A***) Elimination of bla_{TEM}-1gene in the retentate and permeate. (***B***) Elimination of *acc(3)-II* gene in the retentate and permeate. (***C***) Elimination of genetic mobile element (*Intl1*) in the retentate and permeate.

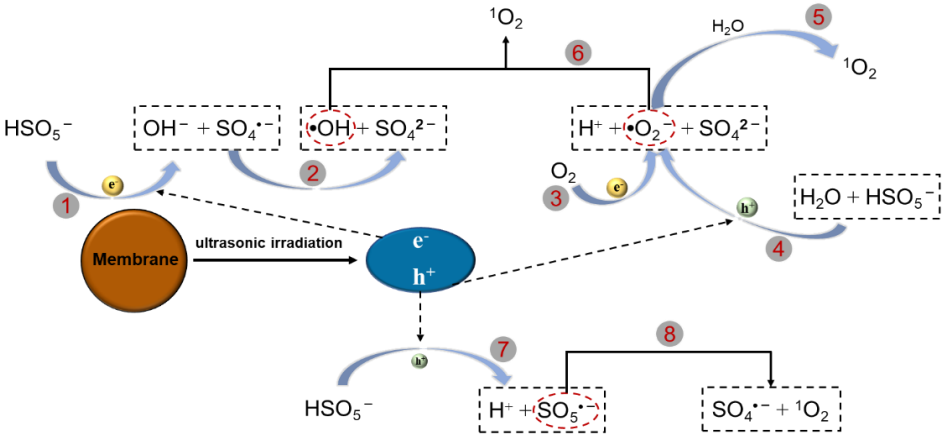

Pathway 1: Membrane + US → e^- + h^+

Pathway 2: HSO_5^- + e^- → •OH + SO_4^{2-}

Pathway 3: O_2 + e^- → $\bullet O_2^-$

Pathway 4: HSO_5^- + H_2O → H^+ + $\bullet O_2^-$ + SO_4^{2-}

Pathway 5: $\bullet O_2^-$ + H_2O → $^1O_2$ + OH^-

Pathway 6: $\bullet O_2^-$ + •OH → OH^- + $^1O_2$

Pathway 7: HSO_5^- + h^+ → H^+ + $SO_5^{\bullet-}$

Pathway 8: $SO_5^{\bullet-}$ → $SO_4^{\bullet-}$ + $^1O_2$

Supplementary Figure 19. Pathways for ROS generation in the piezoelectric PMS activation during PTFE-ZnO nanofiber membrane filtration.

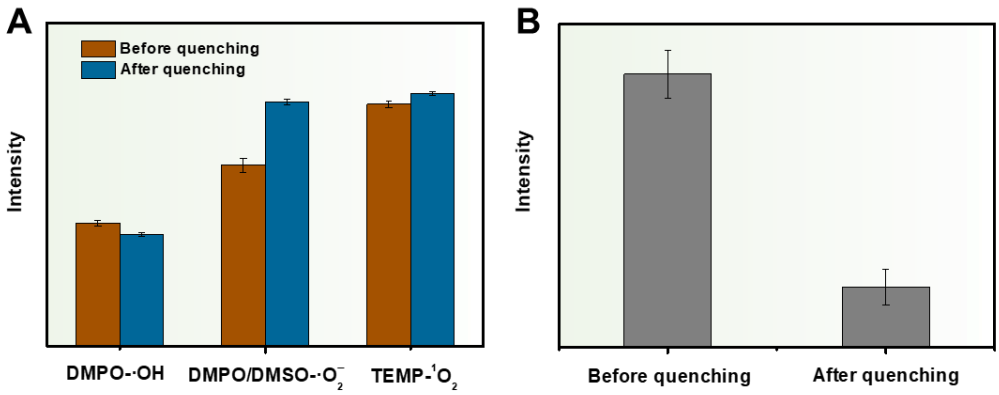

Supplementary Figure 20. ESR signal intensity before and after quenching. (***A***) Intensity of DMPO-•OH, DMPO/DMSO-•O_2^- and TEMP-$^1O_2$ after the quenching of piezo-induced electron (e^-). (***B***) Intensity of TEMP-$^1O_2$ after the quenching of •OH and •O_2^-.

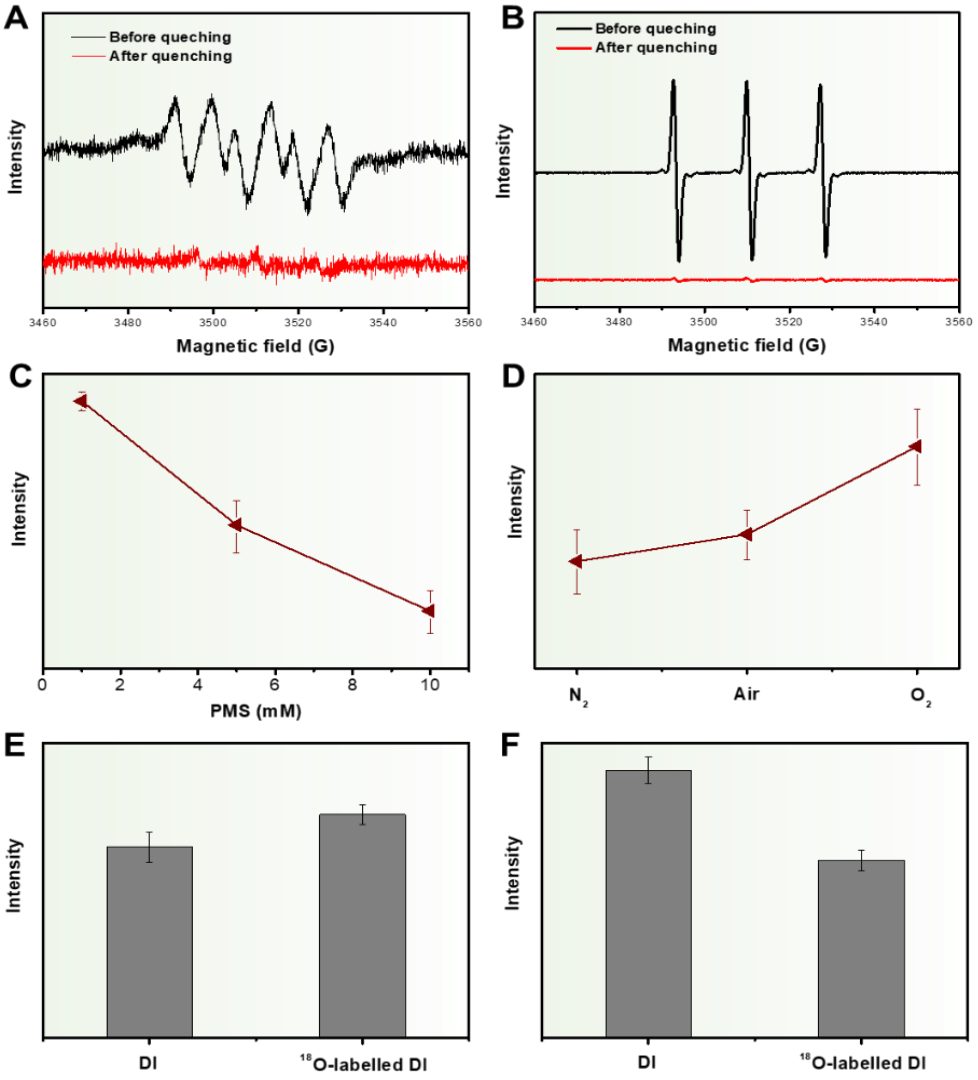

Supplementary Figure 21. ESR signal intensity of DMPO-•OH, DMPO/DMSO-•O_2^- and TEMP-$^1O_2$. (***A***) Intensity of DMPO/DMSO-•O_2^- after the quenching of piezo-induced hole. (***B***) Intensity of TEMP-$^1O_2$ after the quenching of piezo-induced hole (h^+). (***C***) Intensity of DMPO/DMSO-•O_2^- with different PMS concentrations. (***D***) Intensity of DMPO/DMSO-•O_2^- with different dissolved O_2 concentrations. (***E***) Intensity of DMPO/DMSO-•O_2^- with the addition of 50wt% ^{18}O-labelled DI. (***F***) Intensity of TEMP-$^1O_2$ with the addition of 50wt% ^{18}O-labelled DI.

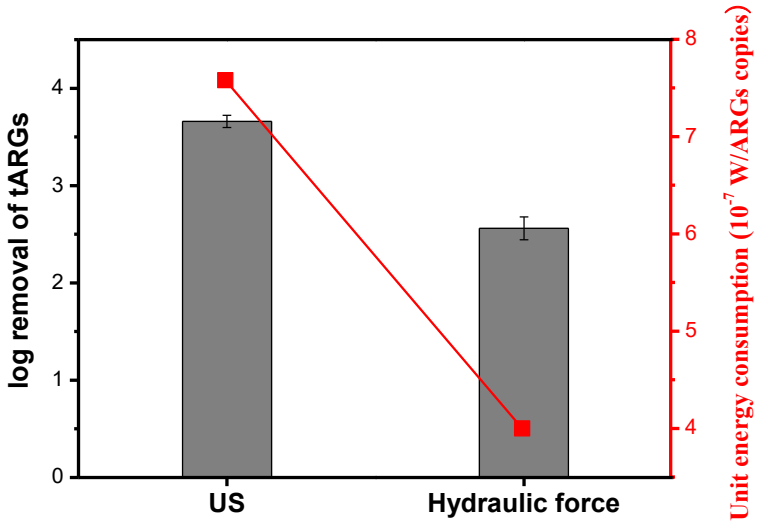

Supplementary Figure 22. A comparison in the tARGs removal and unit energy consumption between US-driven and hydraulic-driven pieozoeletric membrane filtration.

Supplementary Tables

Supplementary Table 1. Chemical composition of electrospinning solutions.

Nanofiber membrane	PTFE aqueous dispersion (60wt%, mL)	PEO (g)	ZnO (g)	DI (mL)
PTFE	20	0.78	--	9.22
PTFE-ZnO	20	0.78	0.12	9.10

Supplementary Table 2. Water flux, hydrophilicity and porosity of the membranes

Nanofiber membrane	Water flux ($L \cdot m^{-2} \cdot h^{-1} \cdot bar^{-1}$)	Water contact angle (°)	Total porosity (%)
PTFE	102.4	132.4	48.4
PTFE-ZnO	115.7	110.2	45.3

Supplementary Table 3. Rejection of ARB and plasmids pUC57 encoded with *bla*$_{TEM}$-1 by PTFE-ZnO nanofiber membrane.

Target	Initial concentration	log removal	Removal percentage (%)
ARB	~10^7 CFU·mL^{-1}	-0.1993	36.8
Plasmid	~10^7 copies·mL^{-1}	-0.0047	1.08

Note: ARB or plasmid solution was quickly filtered through PTFE-ZnO nanofiber membrane using syringe filter.

Supplementary Table 4. The k_{obs} values of ARGs degradation reported in previous studies.

Catalyst [Ref.]	ARB suspension	Oxidant: dosage (mM)	Efficiency	k_{obs} (min^{-1})
nZVI [5]	~10^8 CFU·mL^{-1} *E. coli* with *bla*$_{TEM}$-1	PS: 1.0	~2 log removal of iARGs in 30 min	0.43
S-Nzvi [5]	~10^8 CFU·mL^{-1} *E. coli* with *bla*$_{TEM}$-1	PS: 1.0	~4 log removal of iARGs in 60 min	0.60
ZVI [6]	~10^7 copies·mL^{-1} *P. putida* MX-2 with *acrB*, *tetA*-02, *sulI*, *mexF*, *tetA-01, aac6-lb,* and *str*A	PS: 2.0	2.01-3.21 log removal of ARGs in 90 min	0.02-0.03
UV [7]	~10^7 copies·mL^{-1} plasmid with *bla*$_{NDM}$-1	PMS: 0.03	~2 log removal of ARGs in 10 min	0.22
UVC [8]	~10^8 CFU·mL^{-1} *Pseudomonas sp.* HLS-6 with *sul1*	PMS: 0.03	2.9 log removal of ARGs in 30 min	0.47
FeS_2@GO [9]	~10^6 CFU·mL^{-1} *E. coli* with *bla*$_{TEM}$-1	H_2O_2: 1.0	~1.3 log removal of iARGs in 30 min	N/A
Co_3O_4-SiO_2 [10]	~10^7 CFU·mL^{-1} *Pseudomonas sp.* HLS-6 with *sul1*	PMS: 0.03	~4.0 log removal of ARGs in 60 min	~0.07
N.A. [11]	~10^8 CFU·mL^{-1} *E. coli* with *tetA*	PMS: 0.08	1.09 log removal of ARGs in 30 min	N/A
Electrified CNT membrane [12]	~10^5 copies·mL^{-1} *sulI* gene in *Pseudomonas* sp. *HLS-6* and ~10^7 copies·mL^{-1} *tetA* gene in *E. coli*	NaClO: 0.02	4.6 log removal of *sulI* and 1.7 log removal of *tetA* in 30 min	N/A
PTFE-ZnO nanofiber membrane	~10^7 CFU·mL^{-1} *E. coli* with *bla*$_{TEM}$-1	PMS: 1.0	~0.50 log for iARGs and ~0.14 log for eARGs in 9 min (zone 1)	0.12
			~2.97 log for iARGs and ~1.78 log for eARGs in 0.2 min (zone 1)	34.1

N/A: value unavailable.

Supplementary References

1. Wang, Y.; Xu, Y.; Dong, S.; Wang, P.; Chen, W.; Lu, Z.; Ye, D.; Pan, B.; Wu, D.; Vecitis, C.D.; Gao, G. Nat. Commun. **2021**, *12*, 3508.
2. Wen, Y.; Chen, J.; Gao, X.; Liu, W.; Che, H.N.; Liu, B.; Ao, Y.H. Nano Energy **2023**, *107*, 108173.
3. Zhu, M.; Chen, X.Q.; Tang, Y.; Hou, S.; Yu, Y.; Fan, X.Y. J. Hazard. Mater. **2022**, *437*, 129359.
4. Chen, C.; Wang, Y.Y.; Huang, Y.J.; Hua, J.; Qu, W.; Xia, D.H.; He, C.; Sharma, V.K.; Shu, D. Appl. Catal. B Environ. **2023**, *321*, 122062.
5. Yu, Z.; Rabiee, H.; Guo, J.H. Water Res. **2021**, *198*, 117141.
6. Meng, X.; Li, H.; Yan, S.; Ning, Z.P.; Yuan, Q.; Liu, C.S.; Zhou, L.X.; Zheng, G.Y. Chem. Eng. J. **2023**, *452*, 139413.
7. Yao, S.; Hu, Y.; Ye, J.F.; Xie, J.H.; Zhao, X.T.; Liu, L.L.; Lyu, S.G.; Lin, K.F.; Cui, C.Z. Chem. Eng. J. **2022**, *433*, 133565.
8. Hu, Y.; Zhang, T.Y.; Jiang, L.; Yao, S.J.; Ye, H.; Lin, K.F.; Cui, C.Z. Chem. Eng. J. **2019**, *368*, 888-895.
9. Ahmed, Y.; Zhong, J.X.; Wang, Z.L.; Wang, L.Z.; Yuan, Z.H.; Guo, J.H. Environ. Sci. Technol. **2022**, *56*, 15156-15166.
10. Tian, Y.; Yao, S.J.; Zhou, L.; Hu, Y.; Lei, J.Y.; Wang, L.Z.; Zhang, J.L.; Liu, Y.D.; Cui, C.Z. J. Hazard. Mater. **2022**, *430*, 127414.